



3D Hydrodynamic Modeling of Sediment Dynamics on Roberts Bank, Fraser River Foreslope, Strait of Georgia, Canada

Jianhua Jiang¹ and David B. Fissel¹

Presented at ECM9, Charleston, SC, 2005

Abstract

A fully three-dimensional, nested grid, integrated circulation-wave-sediment-geomorphology numerical model, COCIRM-SED, was developed to study sediment dynamics on Roberts Bank, Fraser River foreslope, Strait of Georgia, Canada. Roberts Bank is an extensive intertidal zone, located just south of where the main (South Arm) Fraser River channel enters the Strait of Georgia. The substrate of Roberts Bank is primarily silty sand, and a total of four grain size classes were considered in the model. The study area of interest is modeled using a fine grid size of 100 m by 100 m, and is nested within the much larger domain of the Strait of Georgia with a coarser grid size of 500 m by 500 m. These two model domains are solved together at every time step using a fully dynamic and two-way connection scheme. Following initial testing with idealized analytical cases, the COCIRM-SED modeled flows and suspended sediment concentration were calibrated and verified using the data obtained with a configurable multi-sensor tripod system on the Bank and at the edge of the Bank, respectively. These field data, including month-long ADCP current profiles, OBS sediment concentrations, and directional wave measurements, are used to examine the model performance. The preliminary model results provide improved understandings of the sediment dynamics on Roberts Bank.

Introduction

River deltas and associated foreslopes develop at river mouths having high fluvial sediment loads, generally exceeding 0.2 kg/m^3 (Friedman and Sanders, 1978). These regions play very important roles both ecologically and geologically in the entire river, estuarine and coastal environmental system (Stanley, 2001). Due to dense population and heavy human activities, such as port facilities, dredging, training projects of navigation channels, and fresh water diversion for urban and agriculture uses, the dynamic nature of sediment transport and the delta and foreslope modern development processes have been highly modified and adversely impacted (Vaughn and Currie, 2000; Wang, et al., 2003).

The increasing human needs have given rise to the challenge of addressing sustainable uses of river foreslope and deltas. To minimize human impacts requires fully understanding such physical processes over river foreslopes and deltas as river discharge and sediment load, tidal currents, waves, drying/wetting, sediment transport

¹ASL Environmental Sciences Inc., 1986 Mills Rd., Sidney, BC, V8L 5Y3, Canada, jjiang@aslenv.com and dfissel@aslenv.com

and morphodynamics. In the past decade, numerical models have become more and more robust and reliable tools for scientists and engineers in reproducing and predicting these physical processes (e.g., Cheng, et al., 1993; Woolnough, et al., 1995; Wood and Widdows, 2002). However, accurate implementation of numerical models remains a great challenge because of complex dynamics and sediment properties, and high resolution demands for model grids over these regions.

This study is thus intended to develop a useful approach for numerical modeling of sediment dynamics for an integrated river, estuarine and coastal environmental system. The numerical model is fully three-dimensional, starts from the framework of an existing coastal circulation model, COCIRM, and couples together new modules for waves, cohesive and non-cohesive sediment transport based on multiple size classes, and geomorphology. Consistent with the previous acronym, the newly-developed 3D numerical model is called COCIRM-SED. Extensive model validation experiments are ongoing, and this paper briefly describes the approaches used in developing this model and presents preliminary results of its implementation.

Overview of COCIRM-SED

COCIRM-SED consists of four integrated modules (Figure 1): circulation, wave, sediment transport and morphodynamics. The circulation module (COCIRM), developed over the past several years (Jiang, 1999; Fissel, et al., 2002; Jiang, et al., 2003; Jiang and Fissel, 2004), represents a computational fluid dynamics approach to the study of river, estuarine and coastal circulation regimes. The wave module is an adaptation of the third generation, nearshore transformation spectral wave model, SWAN, developed by the Delft University of Technology. The sediment transport model involves the dynamics of cohesive and non-cohesive sediment based on multiple size classes. The morphological module solves the bottom elevation variations due to sediment deposition and erosion over different periods. The model explicitly simulates such natural forces as pressure heads, buoyancy or density difference due to salinity, temperature and suspended sediment, river inflow, meteorological forcing, and bottom and shoreline drag. The model applies the fully three-dimensional basic equations of shallow water hydrodynamics and conservative mass transport combined with a second order turbulence closure model (Mellor and Yamada, 1982), where the pressure is simply assumed hydrostatic, then solves for time-dependent, three-dimensional velocities, salinity, temperature, suspended sediment concentrations and coarse sediment bed-loads by size category, turbulence kinetic energy and mixing length, horizontal and vertical diffusivities, water surface elevation, 2D wave spectra, wave forces, and bottom elevation variations.

A semi-implicit finite difference method is applied in COCIRM-SED. This numerical solution has the advantage of good stability. The stable time step, dt , is only restricted by horizontal diffusivity as follows (Casulli and Cheng, 1992)

$$dt \leq \text{MIN} \left[2(A_x, A_y) \left(\frac{1}{dx^2} + \frac{1}{dy^2} \right) \right]^{-1} \quad (1)$$

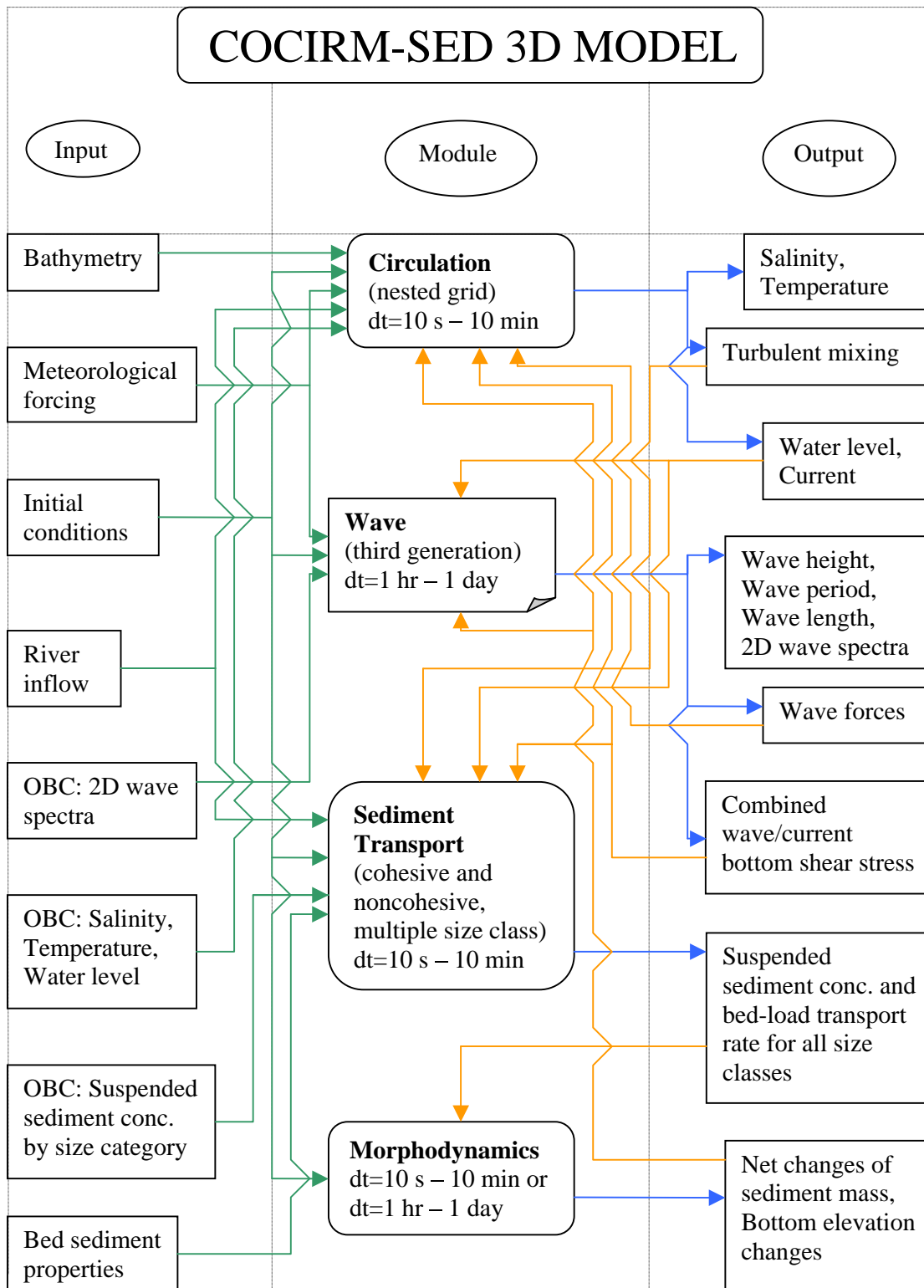


Figure 1: Schematic Diagram of COCIRM-SED system.

where A_x and A_y are respectively horizontal diffusion coefficients in x- and y-directions, and dx and dy are spatial grid sizes in x- and y-directions, respectively. Evidently, when $A_x = A_y = 0$, this scheme becomes unconditionally stable. The model is incorporated with a drying/wetting scheme and is capable of modeling circulation, wave and sediment dynamics over intertidal zones. By using a fully dynamic and two-way connection nested grid approach (Jiang, et al., 2003), the model also allows a high grid resolution refinement, up to a factor of 1/20, in particular area of interest to coastal engineering project and having high resolution demand. The horizontal grid sizes are typically in the range of 5 m to 1,000 m. The vertical sigma-grid may be distributed evenly or with log-resolution near surface and bottom and linear in between, with typically 10 – 20 layers.

To activate the sediment transport and morphological modules, one need only input the grain size (d_k) and percentage fraction (f_k) for each sediment category, with a typical total number of categories 5 – 20. COCIRM-SED readily simulates settling velocities (w_k), suspended sediment concentration (c_k), bed-load rates ($S_{b,k}$), and bottom elevation changes by size category. For fine-grained sediments with particle size less than 32 – 62 μm (clay – silt range), modeling of cohesive sediment transport will be involved, while for coarse sediments with particle size greater than 32 – 62 μm (sand, granule and fine pebble), modeling of non-cohesive sediment transport will be activated.

For cohesive sediments, bottom deposition, D_k (Krone, 1962), erosion, E_k (Parchure and Mehta, 1985), and settling velocity, w_k (Mehta and Li, 1997) are given by

$$D_k = w_{s,k} c_k H \left[1 - \frac{\tau_{cw}}{\tau_d} \right] \left(1 - \frac{\tau_{cw}}{\tau_d} \right) \quad (2)$$

$$E_k = f_k M_{\max} \exp(-\chi \tau_e^\lambda) H[\tau_{cw} - \tau_e] (\tau_{cw} - \tau_e) \quad (3)$$

$$w_{s,k} = \left[\frac{ac_k^\alpha}{(c_k^2 + b^2)^\beta} \right] \left[\frac{\rho_{s,k} / \rho(\theta, s, c) - 1}{1.65} \right] \left[\frac{10^{-6}}{\nu(\theta, c)} \right] F(\theta) \quad (4)$$

where $H[-]$ is a heavyside function which becomes zero if the quantity inside the square brackets becomes negative, otherwise is equal to one, τ_{cw} is the bottom shear stress due to current and wave (Grant and Madsen, 1979), τ_d is the critical shear stress for deposition, which is taken as 0.1 N/m² (Krone, 1962), τ_e is the critical shear stress for erosion, M_{\max} is the maximum erosion constant at $\tau_{cw} = 2\tau_e$, χ , λ , a , b , α and β are the sediment-dependent empirical coefficients, θ is the temperature, $\rho_{s,k}$ is the sediment granular density of kth sediment, $\rho(\theta, s, c)$ is the temperature, salinity and sediment dependent fluid density, $\nu(\theta, c)$ is the temperature and sediment dependent fluid viscosity, and $F(\theta)$ is the temperature effect function on flocculation, $F(\theta) = 1.777 - 0.0518\theta$, for $\theta = 0 - 30$ °C (Jiang, 1999). Two types of cohesive sediment

beds are classified, namely newly-deposited and fully-consolidated beds. The newly-deposited bed goes through consolidation process (Toorman and Berlamont, 1993), while the dry weight for the fully-consolidated bed is simply computed using empirical profile formula. The shear strength of the bottom cohesive sediments is then calculated in terms of solid weight fraction as follows (Mehta, 1991).

$$\tau_e = \tau_{e0} + \alpha_1 (\phi - \phi_c)^{\beta_1} \quad (5)$$

where τ_{e0} is the shear strength for newly deposited sediment, α_1 and β_1 are sediment-dependent coefficients, ϕ is the solid weight fraction ($= c_k / \rho_{s,k}$), ϕ_c is the critical solid weight fraction below which mud has a fluid-like consistency.

For non-cohesive sediments, the effect of particle interaction on settling velocities is considered as follows

$$w_k = \left(1 - \frac{c}{\rho_{s,k}} \right)^4 w_{k0} \quad (6)$$

where c is the total suspended sediment concentration, and w_{k0} is the free settling velocity. By assuming spherical particles, the Stokes law is a fairly good approximation of free settling velocity with Reynolds number $Re < 0.5$ ($Re = w_{k0} d_k / \nu$). For higher Reynolds number, the effects of inertia and virtual mass have to be accounted for. Due to the effect of flow separation behind the falling particle, the value of the drag coefficient depends strongly on the level of free stream turbulence, apart from turbulence caused by the particle itself. In this case, the formulas reported in van Rijn (1984a) are applied. Two separated parts are involved in coarse sediment transport, namely suspended-load and bed-load. The formulas introduced in van Rijn (2000) are used for calculating the bed-load transport rates. For suspended-load transport, the bottom sediment re-suspension and deposition are given by

$$\begin{aligned} E_k &= c_{a,k} \left(\frac{K_v}{\Delta z} \right) \\ D_k &= c_{1,k} \left(\frac{K_v}{\Delta z} + w_k \right) \end{aligned} \quad (7)$$

where K_v is the vertical diffusion coefficient at the bottom of the lowest σ -layer, which is derived from the second order turbulence closure model, Δz is the vertical distance from the reference level a to the center of the lowest σ -layer, $c_{1,k}$ is the k^{th} sediment concentration at lowest σ -layer, and $c_{a,k}$ is the sediment reference concentration at the reference level a , which is determined from (van Rijn, 1984b)

$$c_{a,k} = 0.015 f_k \eta_k \rho_{s,k} \frac{d_k^{0.7}}{a} \frac{\left[(u_* / u_{*k})^2 - 1 \right]^{1.5}}{\left[(\rho_{s,k} / \rho - 1) g / \nu^2 \right]^{0.1}} \quad (8)$$

where η_k is the user-specified calibration parameter for k^{th} sediment, u_* is the shear velocity due to current and wave, g is the gravitational acceleration, and $u_{*,k}$ is the critical shear velocity for incipient motion of k^{th} sediment. In determining $u_{*,k}$, the hiding and exposure factor of non-uniform coarse sediment bed is taken into account due to the work by Wu, et al. (2000) as follows

$$u_{*,k} = \left[\left(\frac{\rho_{s,k}}{\rho} - 1 \right) g d_k \mathcal{G}_c \left(\frac{p_{h,k}}{p_{e,k}} \right)^m \right]^{0.5} \quad (9)$$

where \mathcal{G}_c is the non-dimensional critical shear velocity corresponding uniform sediment or the mean size of bed materials, m is the empirical constant ($\cong 0.6$), and $p_{h,k}$ and $p_{e,k}$ are respectively the total hidden and exposed probabilities of k^{th} non-cohesive sediment.

In the morphological module, an acceleration factor, f_m (≥ 1.0), is introduced in dealing with time scale difference between hydrodynamics and morphodynamics. The bottom elevation changes at any model grid cell (i,j) is given by

$$\Delta h_{i,j} = \sum \left[(\Delta S_{bed})_{i,j} + (\Delta S_{sus})_{i,j} \right] f_m dt \quad (10)$$

where $(\Delta S_{bed})_{i,j}$ is the ratio of bed-load rate net change into or out off the model grid cell (i,j) to the dry weight of bottom sediment, $\rho_{d,k}$, and $(\Delta S_{sus})_{i,j}$ is the ratio of net bottom erosion and deposition to the dry weight of bottom sediment, and is determined by

$$(\Delta S_{sus})_{i,j} = \sum_{k=1}^K \frac{(D_k - E_k)_{i,j}}{\rho_{d,k}} \quad (11)$$

where K is the total number of sediment fractions.

Module Integration and Coupling

COCIRM-SED was developed in a fashion that carefully integrates and couples sub-modules together within the same computational framework, except the wave module SWAN, which runs externally (Figure 1). Changes in wave conditions occur over time scales of hour to days while circulation and sediment dynamics can have shorter time scales, and moreover, modeling spectral wave transformations has a very high demand on computer physical memory. It is hence more economic and efficient to run the wave model SWAN externally and input the simulated wave parameters (e.g., wave forces, significant wave height, wave period, wave length and wave direction) into COCIRM-SED. At every time step, COCIRM-SED interpolates wave parameters from the output of SWAN, and inputs them to other modules. The buoyancy effects due to salinity, temperature and suspended sediments on the

circulations are all taken into account, and the state function of the bulk density of water is read as follows

$$\rho(\theta, s, c) = \rho_0(\theta, s) + \sum_{k=1}^K \left(1 - \frac{\rho_0(\theta, s)}{\rho_{s,k}} \right) c_k \quad (12)$$

where $\rho_0(\theta, s)$ is water density under the effect of salinity and temperature. The feedback of morphodynamics to other physical processes is made possible by changing the bottom elevation derived from Eq. (10) at every time step.

Initial Results of Implementations

Dredged Trench Migration under Effect of Current

Before modeling the Fraser River foreslope sediment dynamics, COCIRM-SED was tested for number of idealized cases, which include (1) suspended sediment equilibrium profile under the effect of stationary and uniform current, (2) development of suspended sediment transport under the effect of stationary and uniform currents, (3) non-equilibrium profiles of suspended cohesive sediment under the effect of stationary and uniform currents, (4) suspended sediment equilibrium profile under the effect of stationary and uniform currents and waves, (5) equilibrium profiles of multiple grain size sediments under the effect of stationary and uniform currents and waves, and (6) dredged trench migration under the effect of currents. Testing results for cases 1 – 5 were compared with available analytical solutions and other model simulations, and were found to be in excellent agreement (not shown). Case 6 is an application of a flume experiment of dredged trench migration reported in DHL (1980). The model results show that the initially-dredged trench gradually shifted to downstream in such a fashion that is in generally good agreement with the laboratory measurements (Figure 2).

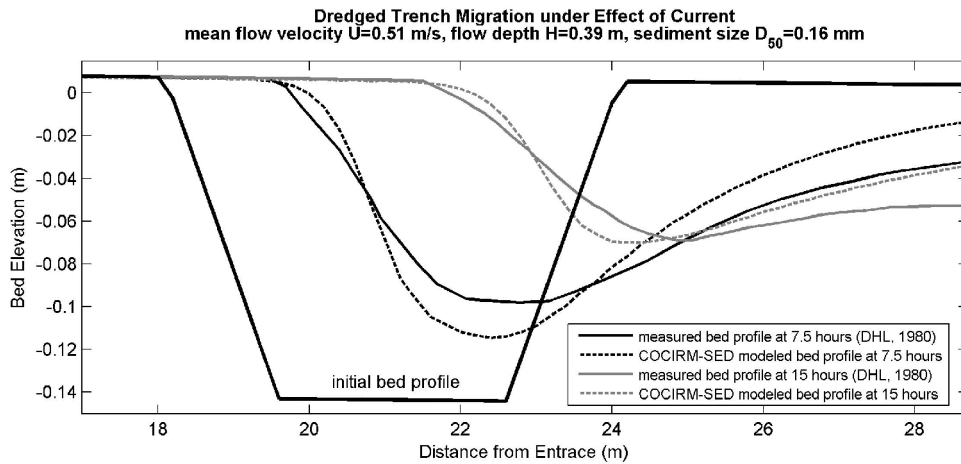


Figure 2. Model results of dredged trench migration, with comparisons to the flume experiment by DHL (1980).

Fraser River Forslope Sediment Dynamics

The COCIRM-SED was then applied to the study of sediment dynamics on Roberts Bank of the Fraser River foreslope, Strait of Georgia, Canada (Figure 3). Roberts Bank is an extensive intertidal zone, located just south of where the main (South Arm) Fraser River channel enters the Strait of Georgia. The substrate of Roberts Bank is primarily silty sand, and a total of four non-cohesive sediment classes were considered in the model in terms of a typical Roberts Bank grain size curve (Anderson, et al., 1977), respectively size 1: 40 μm and 21.6%, size 2: 80 μm and 22.4%, size 3: 120 μm and 30.0%, and size 4: 170 μm and 26.0%. The study area of interest is modeled using a fine grid size of 100 m by 100 m, and is nested within the much larger domain of the Strait of Georgia with a coarser grid size of 500 m by 500 m. These two model domains are solved together at every time step.

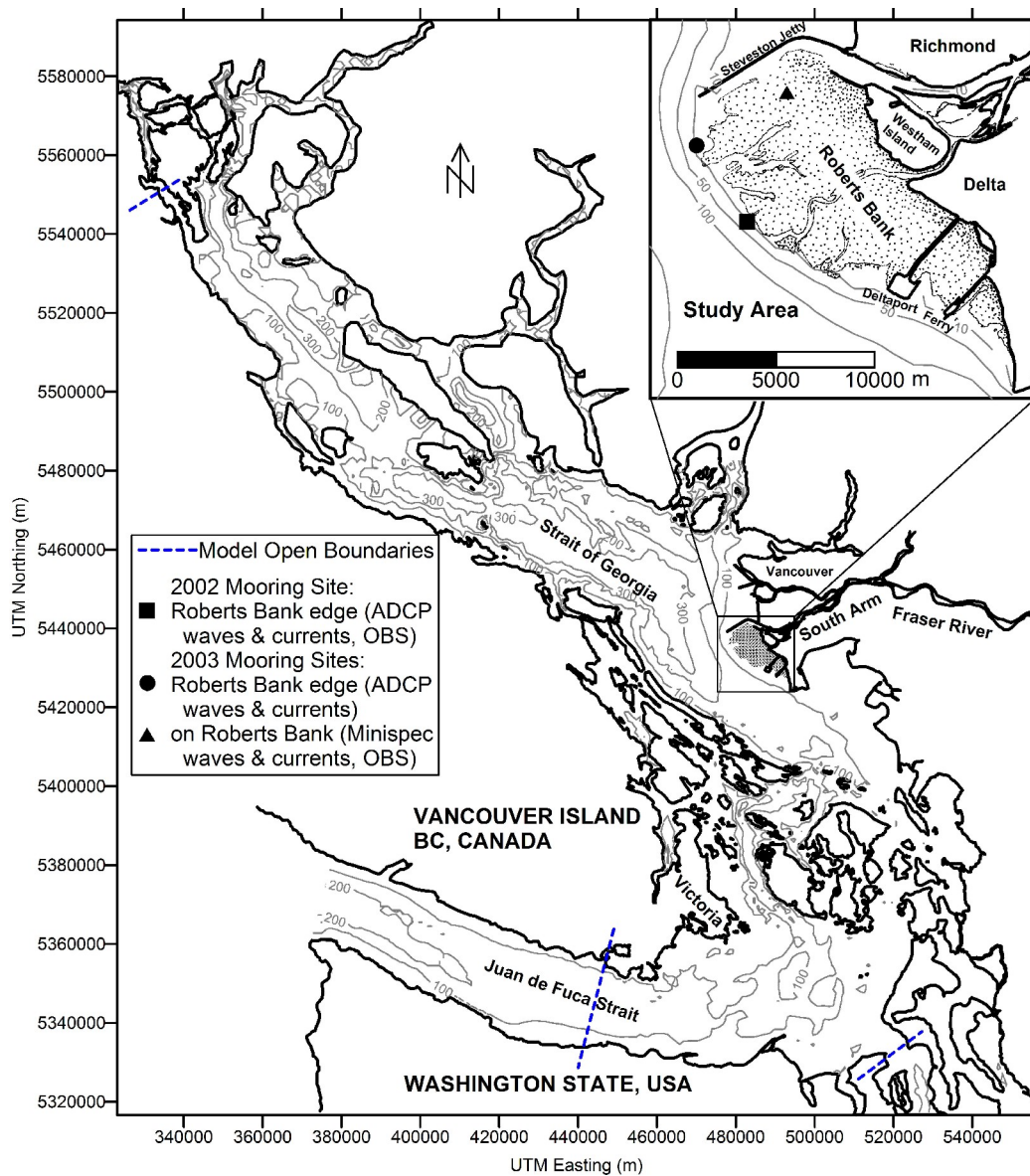


Figure 3. Location map of study area and mooring system sites. Depths are in meters below lowest astronomical tide.

The modeled flows and suspended sediment concentrations were calibrated and verified using the data obtained with a configurable multi-sensor tripod system on the Bank and at the edge of the Bank, respectively. These field data, including month-long ADCP current profiles, OBS sediment concentrations, and directional wave measurements by ASL Environmental Sciences Inc. (Birch, et al., 2002; Birch, et al., 2003a; Birch, et al., 2003b), are used to examine the model performance (Figure 3). Three preliminary model cases have been carried out. These first two cases, with weak wave effects, involved optimization of major physical parameters for circulation and sediment transport, which represents model calibration. The last case retained the optimized parameters and involved stronger wave effects and weaker currents, providing a model verification case.

Calibration Model Results with Negligible Wave Effects

The two calibration cases deal with relatively strong currents and weak wave effects. The first case (C1) ran for a period of 3 days in early March 2002 with a Fraser River discharge of $600 \text{ m}^3/\text{s}$, and the second case (C2) ran for a period of 4.5 days in late April 2003 with a Fraser River discharge of $1,500 \text{ m}^3/\text{s}$. After several trials, the bottom effective roughness height was optimized as 0.0025 m, and the user-specified calibration parameter (η) in Eq. (8) as 0.2 for all sediment size classes.

Model results for C1 are compared with ADCP and OBS observations at the 2002 foreslope edge mooring site (Figure 3). The model currents at three typical levels and water elevations are all in good to very good agreement with observations (Figure 4). The correlation coefficients of modeled versus observed results are 0.79 or better for flow speeds, 0.84 or better for flow directions, and up to 0.99 for water elevations. Noteworthy discrepancies between simulations and measurements only appear near the surface. It is believed that these discrepancies are mainly caused by wind effects, which were not included in current model runs as the winds were generally light during this time of the year.

The comparisons of total suspended sediment concentrations (SSC) between C1 model and OBS at two near bottom levels are shown in Figure 5. It is seen that generally, the simulations are in good agreement with OBS observations, especially those with significant peaks of suspended sediments. For some SSC peaks, the model results are larger, possibly due to near-local model currents being larger and resuspending more sediments. However, for other peaks the model results are lower than observations. During weak currents the model values are generally lower than observations, when SSC values are very low ($< 0.01 \text{ kg}/\text{m}^3$). The data appear to have wash load near the bottom which the model does not represent.

Model results for C2 are compared, respectively, with the data of ADCP at the 2003 foreslope edge mooring site and the data of Minispec and the OBS at the 2003 intertidal (Roberts Bank) mooring site (Figure 3). It is observed that at the foreslope edge mooring site, the comparisons of modeled and observed currents at three typical levels and water elevations (Figure 6) exhibit the same quality as seen in C1. The model currents at deeper levels appear to be in better agreement with observations. The considerable underprediction of flow speed in the middle of the simulated period appears to be a very singular event as compared with observations. Again, it is

believed to be caused by wind effects, which were not included in this model run as winds were generally light during this time of the year.

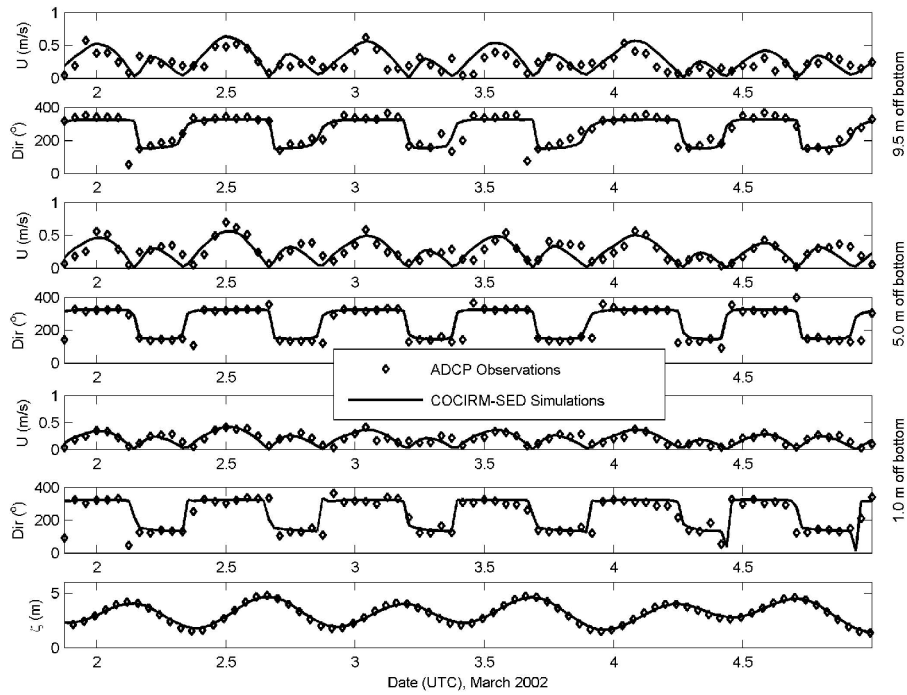


Figure 4. C1 model results of currents for three vertical levels and water elevations at 2002 foreslope edge mooring site, with comparisons to the ADCP observations.

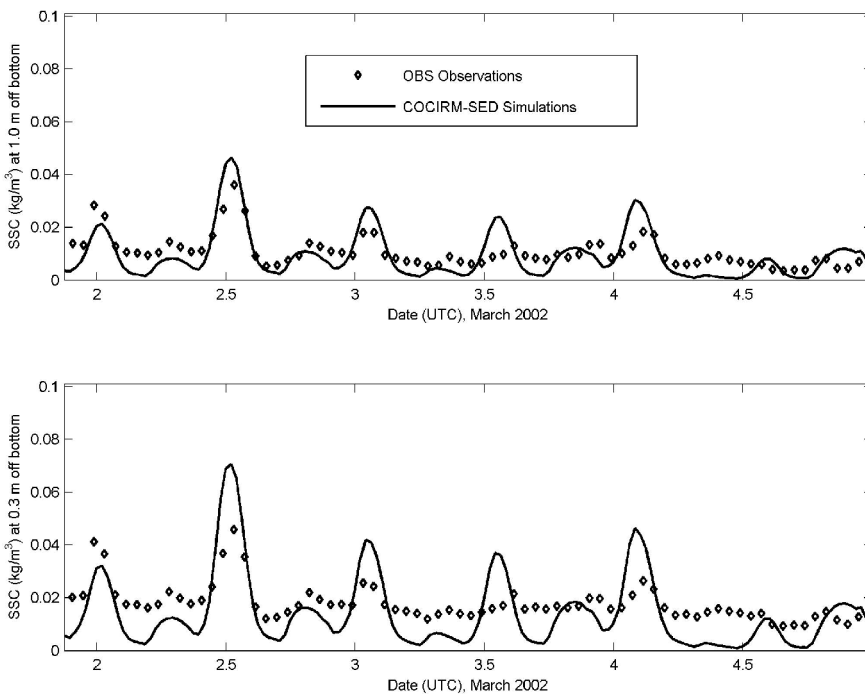


Figure 5. C1 model results of suspended sediment concentrations for two vertical levels at 2002 foreslope edge mooring site, with comparisons to OBS observations.

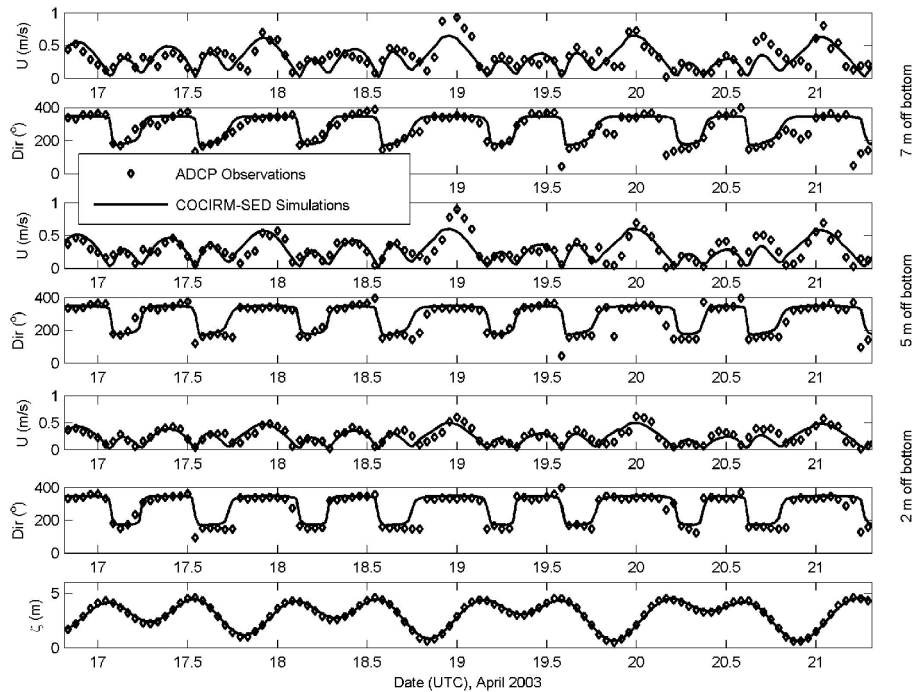


Figure 6. C2 model results of currents for three vertical levels and water elevations at 2003 foreslope edge mooring site, with comparisons to the ADCP observations.

At the intertidal mooring site, the model results of currents and water elevations are in generally good agreement with the observations (Figure 7). Major discrepancies between simulations and observations are noticed during large flood tides, where the model considerably under-predicted the flow speeds as compared with observations. After carefully analyzing the model results and data, it is realized that these discrepancies may be mainly caused by the Roberts Bank bathymetry currently used in the model. From the tidal elevations at the Vancouver reference port reported in the Canadian Tide and Current Tables, 2003, combined with in situ observed water depths, it is found that the actual bottom elevation at the intertidal mooring site is about 0.85 m above the chart datum, while, that in the model is 1.85 m above the chart datum. In other words, the actual bottom elevation at this site is about 1.0 m lower than the one used in the model. The model bathymetries over the Roberts Bank were derived using digitized hydrographic charts by the Canadian Hydrographic Service, which were based on the sounding surveys conducted before 1997 and are most recent bathymetric data available to the public. However, the Roberts Bank tidal flats have been going through substantial human modifications since the construction of the BC Ferry terminal, Vancouver Deltaport and causeways in 60's, and subsequent expansion projects from early 80's to early 90's (Tarbotton, et al., 1993). One of the most significant geomorphological evolutions is the development of dendritic tidal drainage channel network on the Bank (see the enlarged inset for the Roberts Bank in Figure 3), which began with the dredging of borrow pit in 1969 and Deltaport turning basin in 1982. This network is still expanding and has not reached a final equilibrium state (Vaughn and Currie, 2000; VPA, 2005). Therefore, the Roberts Bank bathymetry currently used in the model may not represent the actual ones during the survey in 2003 very well.

The comparisons of total SSC between the model and OBS at 0.3 m and 1.0 m above bottom for the intertidal mooring site are shown in Figure 8. It is seen that the sediment dynamic processes at this site are mainly characterized by three significant SSC peaks each day, respectively during small ebb, large ebb and large flood. The SSC peaks during the small and large ebbs appear both in the model and data, and the modeled and observed results are in generally good agreement, while the SSC peaks during the large floods only appear in the data, and not in the simulations. The later difference is believed to be caused by the Roberts Bank bathymetry currently used in the model. As observed in Figures 7 and 8, the large flood SSC peaks in situ observed at 0.3 m above the bottom occur during the periods when the intertidal mooring site is dry in the simulations. It is thus further confirmed that the actual bottom elevation at this mooring site is lower than the one inputted in the model. As described above, such bathymetry input might be the major reason causing the under-predictions of large flood speeds. As a result, the model did not exhibit any significant local sediment re-suspensions and consequent SSC peaks during the large floods.

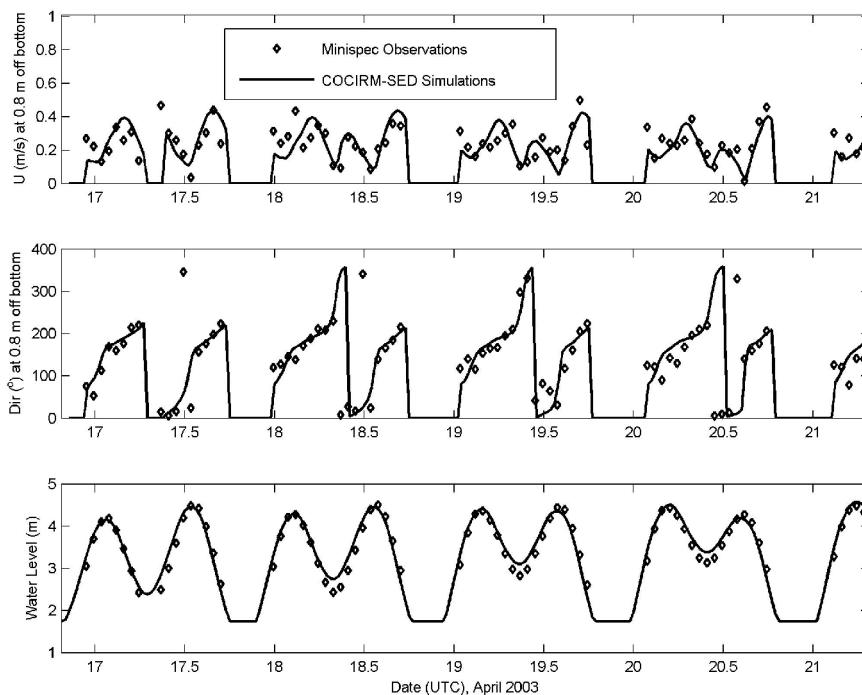


Figure 7. C2 model results of currents and water elevations at 2003 Roberts Bank mooring site, with comparisons to the Minispec observations.

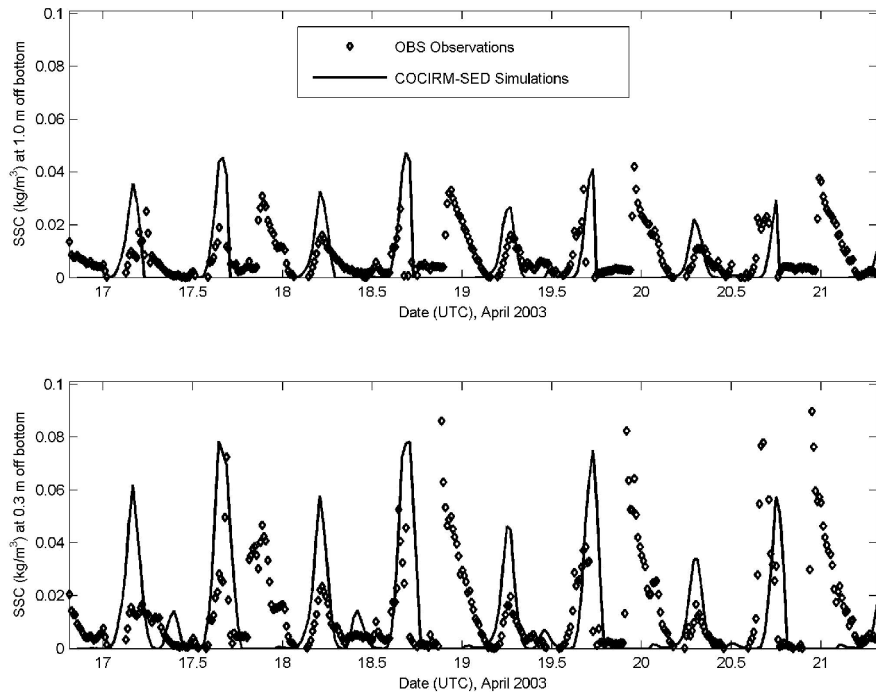


Figure 8. C2 model results of suspended sediment concentrations for two vertical levels at 2003 Roberts Bank mooring site, with comparisons to the OBS observations.

Verification Model Results with Stronger Wave Effects

The verification case deals with neap tides with relatively weak currents. It ran over a period of 2 days at the end of March 2003 with a Fraser River discharge of $1,000 \text{ m}^3/\text{s}$. During this period, a strong wave event occurred, with measured significant wave heights up to 0.7 m at the foreslope edge mooring site (Birch, et al., 2003a). Thus, this model experiment provides an opportunity to assess the model performance of modeling sediment dynamics under wave action.

At first, the wave model SWAN ran externally under local wind generation, and its results of significant wave heights, wave periods, wave directions and wave lengths at all model grids were saved every three hour and inputted into COCIRM-SED. The SWAN outputs of wave heights, periods, and directions at the foreslope edge and intertidal mooring sites were compared with ADCP and Minispec measurements. It was found that the model wave periods and directions are comparable with observations (not shown). The comparisons of the significant wave heights at those two mooring sites are shown in Figure 9. The agreements between simulations and observations are generally good, especially the big wave event in late March 31 and early April 1, which exhibits in both simulations and observations. It is seen that the largest wave in late March 31, which propagated at a direction from 180° (i.e., directed to the north), appears at both mooring sites, while the largest wave on early April 1, which propagated at a direction from 300° , only appear at the foreslope edge. The later feature occurred because the intertidal mooring site happened to be located in the shadowing area of the Steveston Jetty (Figure 3).

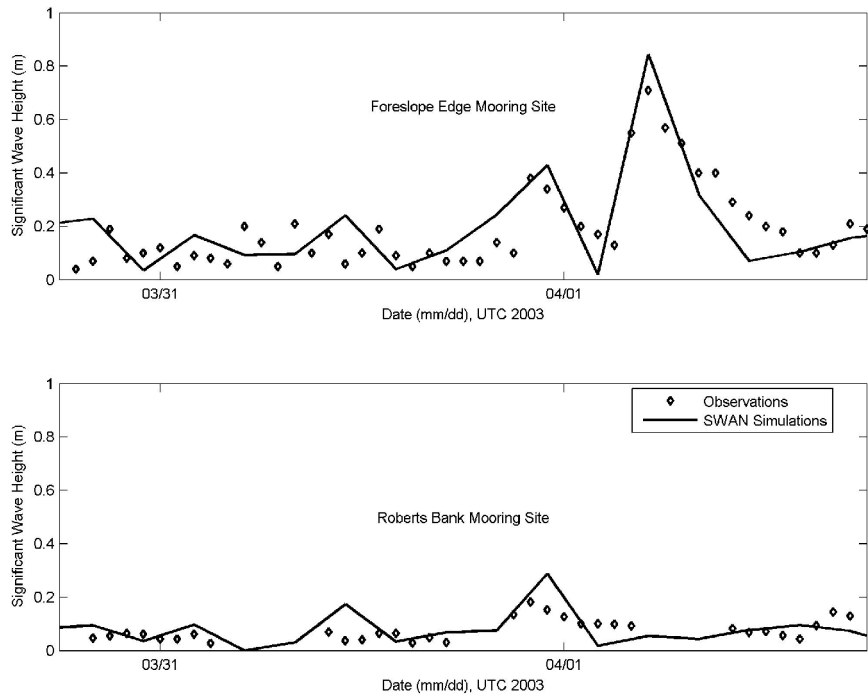


Figure 9. SWAN model results (V1) of significant wave heights at 2003 foreslope edge and Roberts Bank mooring sites, with comparisons to the observations.

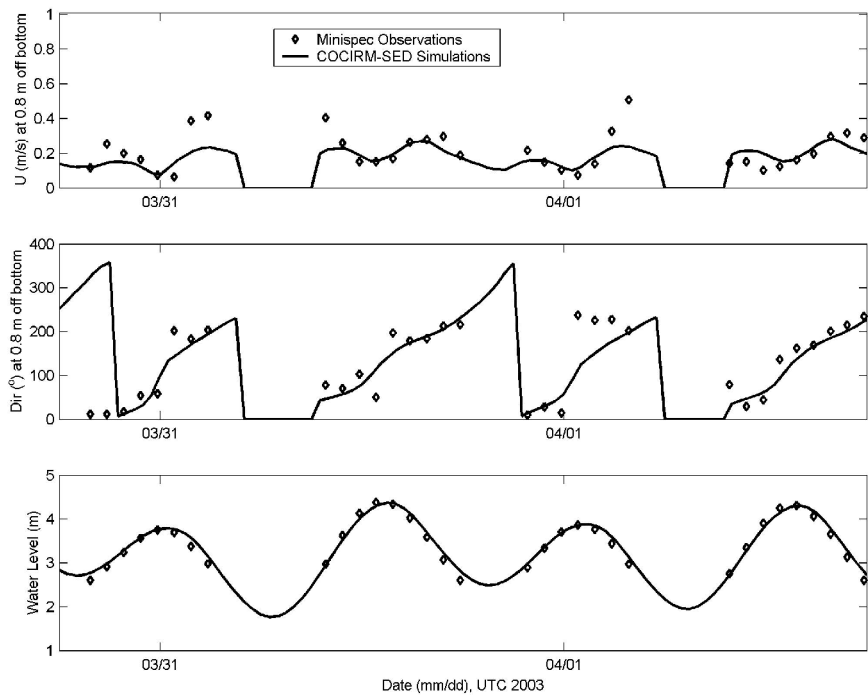


Figure 10. V1 model results of currents and water elevations at 2003 Roberts Bank mooring site, with comparisons to the Minispec observations.

The comparisons between modeled and observed currents and water levels at the foreslope edge mooring site exhibit the same quality as seen in C1 and C2 cases

(not shown). The model results of currents and water levels at the intertidal mooring site are in generally good agreement with observations, and again, the comparisons exhibit the same quality as seen in C2 case (Figure 10). It is observed that the current speeds at 0.8 m above bottom are mostly less than 0.2 m/s, which is lower than 0.25 m/s threshold velocity for re-suspension of silty sand (Birch, et al., 2003b). Consequently, very minor re-suspension and SSC peaks are observed in both model and data, as seen in Figure 11. It is also found that the model SSC at two near-bottom levels are comparable with observations, and the significant sediment re-suspension and SSC peaks during the large wave event are very evident in both model and data (Figure 11), which are apparently induced by wave actions. However, the difference between the modeled and observed results appears to be quite significant in terms of appearance phases of SSC peaks. But, the model results show that the modeled suspended sediments are entirely related to the wave conditions derived from SWAN, which maximum wave height in late March 31 delayed by about one hour compared to the observed one. It is also found that the modeled wave periods are considerably lower than observations (not shown). Therefore, further investigations of wave model results and wind field data (which are the major local generation forcing for waves) are essential in order to improve the model performance.

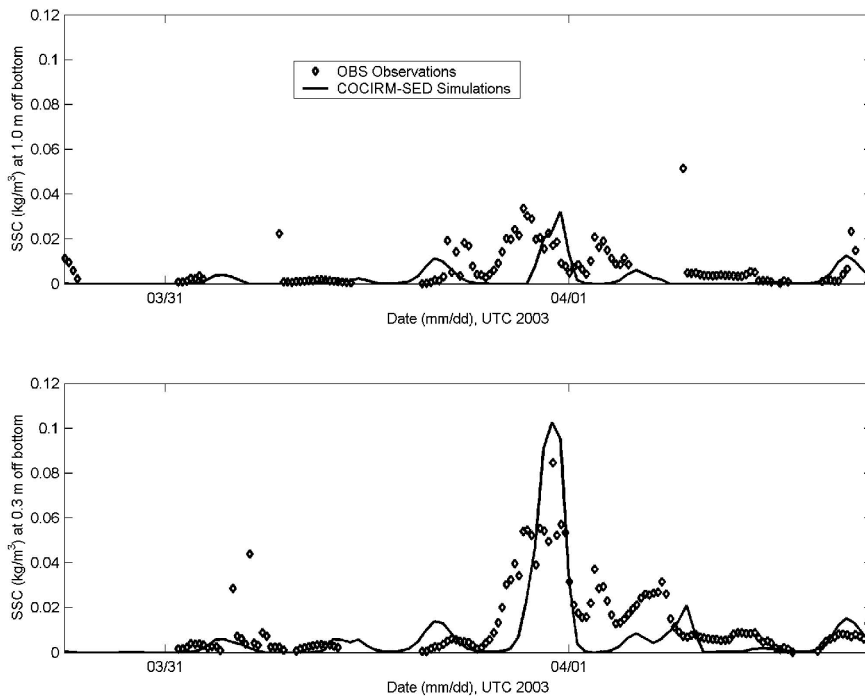


Figure 11. V1 model results of suspended sediment concentrations for two vertical levels at 2003 Roberts Bank mooring site, with comparisons to the OBS observations.

Summary and Conclusion

The preliminary testing of the fully three-dimensional, integrated circulation-wave-sediment-geomorphology numerical model, COCIRM-SED, was successfully conducted with the implementations of idealized cases, flume experiment, and Fraser River foreslope sediment dynamics. The testing results have demonstrated that the model is a useful and robust tool in modeling sediment dynamics in river deltaic and

foreslope regions. More applications of this model are underway, such as modeling the plume off the Fraser River mouth and Roberts Bank long-term geomorphological process, and it is expected that the model capability will be further enhanced through the process of additional calibration and verification runs.

COCIRM-SED was developed in a fashion that carefully integrates and couples all together such physical processes as river discharge and sediment load, tidal currents, salinity, temperature, waves, drying/wetting, sediment transport, and morphodynamics. Meanwhile, it is incorporated with a nested grid and multiple sediment size class schemes. The model thus has the capability of dealing with complex hydrodynamics and sediment dynamics in the river deltaic and foreslope regions. Current preliminary applications of modeling Fraser River foreslope sediment dynamics show that the model results of currents and SSC are in generally good agreement with data obtained with a configurable multi-sensor tripod system on the intertidal zone and at the foreslope edge, respectively. The testing results also show that the model is capable of reproducing sediment re-suspension and consequent SSC peaks under the effect of significant wave event by compared with observations. Major discrepancies between modeled and observed currents and SSC in the intertidal zone are only found during large flood tides, which are believed to be mainly caused by inaccurate Roberts Bank Bathymetry currently available for the measurement location. It is therefore suggested that obtaining and inputting up-to-date Roberts Bank bathymetry is necessary for the next stage of this study.

Acknowledgements

This study has been made possible in part due to the data gathered off the Fraser River delta. The month-long, multi-sensor tripod mooring surveys were funded by the Pacific Geological Survey of Canada and supervised by Dr. Phil Hill and Dr. Gwyn Lintern. Their contributions are most appreciated. We would also like to thank our colleagues at ASL including Rich Birch, Dave English, Vincent Lee, Dave Billenness and Matt Tradewell, who have been involved in providing detailed field measurements and data.

References

Anderson, G.A., Birt, C.S., Johansen, C. and Smyth, T.D. (1977). "*Environmental Assessment of Roberts Bank Port Expansion: Engineering Aspects.*" File 3446, Swan Wooster Engineering Co. Ltd., Vancouver, BC, Canada, 198p.

Birch, R., Lee, V., English, D. and Fissel, D.B. (2002). "*Norton Multiple-Parameter Wave, Current and Sediment Transport Mooring, Fraser Delta Foreslope.*" File 39-482-B, ASL Environmental Sciences Inc., Sidney, BC, Canada, 38p.

Birch, R., Lee, V., Tradewell, M. and English, D. (2003a). "*Sediment Transport Measurements, Roberts Bank, Fraser River Delta.*" File 517 & 520, ASL Environmental Sciences Inc., Sidney, BC, Canada, 53p.

Birch, R., Hill, P.R., Clarke, M., Lemon, D. and Fissel, D.B. (2003b). "*A configurable multi-sensor tripod for the study of near-bottom ocean processes.*" Oceans 2003, San Diego, 1234-1240.

- Casulli, V. and Cheng, R.T. (1992). “*Semi-implicit finite-difference method for three-dimensional shallow water flow.*” *International Journal of Numerical Method in Fluids*, 15, 629-648.
- Cheng, R.T., Casulli, V. and Gartner, J.W. (1993). “*Tidal, residual, intertidal mudflat (TRIM) model and its applications to San Francisco Bay, California.*” *Estuarine, Coastal and Shelf Science*, 36, 235-280.
- DHL (Delft Hydraulics Laboratory), (1980). “*Storm Surge Barrier Oosterschelde, Computation of Siltation in Dredged Trenches.*” Report 1267-V/M 1570.
- Fissel, D.B., Birch, R. and Jiang, J. (2002). “*Three dimensional computational flow modeling and high resolution flow surveys for fisheries environmental studies on the upper Columbia River.*” *Proceedings, Hydrovision 2002, Portland OR, July 2002.*
- Friedman, G.M. and Sanders, J.E. (1978). “*Principles of Sedimentology.*” New York, John Willey and Sons, 792p.
- Grant, W.D. and Madsen, O.S. (1979). “*Combined wave and current interaction with a rough bottom.*” *Journal of Geophysical Research*, 84(C4), 1797-1808.
- Jiang, J. (1999). “*An Examination of Estuarine Lutocline Dynamics.*” Ph. D. dissertation, Coastal & Oceanographic Engineering Department, University of Florida, 226p.
- Jiang, J. and Fissel, D.B. (2004). “*3D Numerical modeling study of cooling water recirculation.*” In: *Estuarine and Coastal Modeling: proceedings of the eighth international conference*, ed. M.L. Spaulding. American Society of Civil Engineers, 512-527.
- Jiang, J., Fissel, D.B. and Topham, D. (2003). “*3D numerical modeling of circulations associated with a submerged buoyant jet in a shallow coastal environment.*” *Estuarine, Coastal and Shelf Science*, 58, 475-486.
- Krone, R.B. (1962). “*Flume Studies of the Transport of Sediment in Estuarial Shoaling Processes.*” *Hydraulic Engineering Laboratory and Sanitary Engineering Research Laboratory, University of California, Berkeley*, 110p.
- Mehta, A.J. (1991). “*Characterization of Cohesive Solid Bed Surface Erosion, with Special Reference to the Relationship between Erosion Shear Strength and Bed Density.*” Report No. UFL/COE-MP-91/4, University of Florida, Gainesville, Florida, 83p.
- Mehta, A.J. and Y. L. (1997). “*A PC-based Short Course on Fine-grained Sediment Transport Engineering.*” Coastal & Oceanographic Engineering Department, University of Florida, 91p.
- Mellor, G.L. and Yamada, T. (1982). “*Development of a turbulence closure model for geophysical fluid problems.*” *Review of Geophysics*, 20(4), 851-875.

- Parchure, T.M. and A.J. Mehta, (1985). "*Erosion of soft cohesive sediment deposits.*" Journal of Hydraulic Engineering, 110, 1308-1326.
- Rijn, van L.C. (1984a). "*Sediment transport, part II: suspended load transport.*" Journal of Hydraulic Engineering, 110, 1613-1641.
- Rijn, van L.C. (1984b). "*Sediment transport, part I: bed load transport.*" Journal of Hydraulic Engineering, 110, 1431-1456.
- Rijn, van L.C. (2001). "*Approximation formulae for sand transport by currents and waves and implementation in Delft-MOR.*" WL | delft hydraulics report Z3054.20.
- Stanley, J.D. (2001). "*Dating modern deltas: progress, problems, and prognostics.*" Annual Review of Earth and Planetary Sciences, 29, 257-294.
- Tarbotton, M., Luternauer, J.L. and Mattila, M. (1993). "*Tidal flat response to development and migration work at Roberts Bank, Fraser River Delta, British Columbia.*" In: Proceedings of the 1993 Canadian Coastal Conference, Vancouver, BC, Canada, 445-457.
- Toorman, E.A. and Berlamont, J.E. (1993). "*Mathematical modeling of cohesive sediment settling and consolidation.*" In: Nearshore Estuarine Cohesive Sediment Transport, A.J. Mehta ed., AGU, Washington D.C., 148-184.
- Vaughn, J. and Currie, R.G. (2000). "*Human impact on sedimentary regime of the Fraser River Delta, Canada.*" Journal of Coastal research, 16(3), 747-755.
- VPA (Vancouver Port Authority), (2005). "Environmental Assessment of Application for the Deltaport Third Berth Project." Vancouver, BC, Canada, p822.
- Wang, Z., Hu, S., Wu, Y. and Shao, X. (2003). "*Delta processes and management strategies in China.*" Intl. J. River Basin Management, 1(2), 173-184.
- Wood, R. and Widdows, J. (2002). "A model of sediment transport over intertidal transect, comparing the influences of biological and physical factors." Limnology and Oceanography, 47, 848-855.
- Wu, W., Wang S. and Jia, Y. (2000). "*Nonuniform sediment transport in alluvial rivers.*" Journal of Hydraulic Research, 38, 427-434.